ACS APPLIED MATERIALS & INTERFACES

Research Article

www.acsami.org

A Facile Synthesis of PEG-Coated Magnetite (Fe_3O_4) Nanoparticles and Their Prevention of the Reduction of Cytochrome C

Anindita Mukhopadhyay,[||,‡] Nidhi Joshi,[||,§] Krishnananda Chattopadhyay,*[,§] and Goutam De*[,‡]

[‡]Nano-Structured Materials Division, Central Glass and Ceramic Research Institute, Council of Scientific & Industrial Research, 196 Raja S. C. Mullick Road, Kolkata 700032, India

[§]Protein Folding and Dynamics Laboratory, Structural Biology and Bioinformatics Division, Indian Institute of Chemical Biology, Council of Scientific & Industrial Research, 4 Raja S. C. Mullick Road, Kolkata 700032, India

Supporting Information

ABSTRACT: We report here a facile and green synthetic approach to prepare magnetite (Fe_3O_4) nanoparticles (NPs) with magnetic core and polyethylene glycol (PEG) surface coating. The interaction of the bare and PEG-coated Fe_3O_4 NPs with cytochrome c (cyt c, an important protein with direct role in the electron transfer chain) is also reported in this study. With ultrasonication as the only peptization method and water as the synthesis medium, this method is easy, fast, and environmentally benign. The PEG coated NPs are highly water dispersible and stable. The bare NPs have considerable magnetism at room temperature; surface modification by PEG has resulted in softening the magnetization. This approach can very well be applicable to prepare biocompatible, surface-modified soft magnetic materials, which may offer enormous utility in the field of biomedical research. Detailed characterizations including XRD, FTIR, TG/DTA, TEM, and VSM of the PEG-coated Fe_3O_4 NPs were carried out in order to ensure the future applicability of this method. Although the interaction of bare NPs with cyt c shows reduction of the protein, efficient surface modification by PEG prevents its reduction.

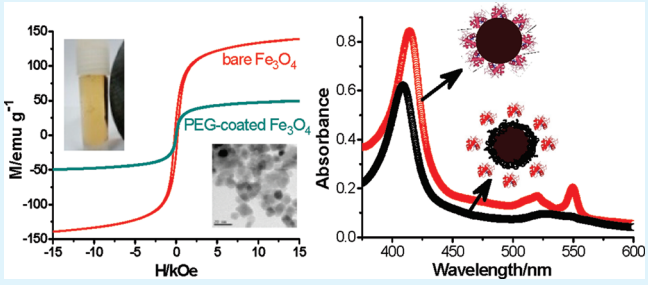

KEYWORDS: *magnetite nanoparticles, polyethyleneglycol−coating, soft magnetic nanomaterials, protein−nanoparticle interaction*

1. INTRODUCTION

Magnetic iron oxide NPs, especially magnetite (Fe_3O_4) and maghemite (γ-Fe_2O_3), have gained considerable attention because of their biocompatibility and use in MRI contrast enhancement[1,2] tissue repair,[3] immunoassay,[4] detoxification of biological fluids,[5] hyperthermia,[6] targeted drug delivery,[7,8] cell separation,[9−11] and so on. As a result, several commercial products based on iron oxide NPs are currently available for human diagnostics. However, the use of magnetite NPs may accompany risks and deleterious effects associated with their increased usage particularly when they are used without appropriate characterization as biological agents.[12−14] It has been known for long that iron, when present in excess in human body, can be associated with carcinogenesis. The presence of iron has also been implicated in the generation of reactive oxygen species (ROS), which can cause direct damage to DNA, proteins or lipid molecules.[15−18] Although iron oxide NPs are generally well-tolerated in vivo, appropriate surface modification, particles size, and core−ligand composition can play definite roles in physiological responses.[19] For these reasons, magnetite NPs are typically surface-modified or coated with biocompatible polymer molecules (e.g., polyvinyl alcohol, dextran, etc.), which improves their colloidal stability in physiological media, reduces toxicity, and significantly increases the blood circulation half-life by minimizing the protein absorption on the NP surface.[20−22] Especially polyethylene glycols (PEGs) of long polymeric chains being highly water-soluble and nontoxic to large extent, have found significant applications in the structure stabilization and delivery of drug biological molecules, which is very much necessary in drug research field.[23−25] Therefore, fabricating any route for an easy and time saving strategy for the synthesis of PEG coated iron oxide NPs would be of utmost importance. Although large number of coating strategies have been applied and appreciated for the PEG-based modifications of magnetic NPs, the synthesis pathway remains more or less complicated so far, requiring the use of special atmospheric conditions.[20,26,30] For example, other functionalizations of PEG with folate receptor, carboxylic acid, or poly(TMSMA-r-PEGMA) modifications have been reported as efficient surface modifiers, where the use of stringent reaction condition as well as nitrogen atmosphere is an essential requirement.[31−35] Literature is also available where a reflux temperature (above 200 °C) has been applied for the synthesis of PEG-coated magnetite nanoparticles.[32] The surface modification procedure described in this paper, on the other hand,

Received: August 30, 2011
Accepted: November 23, 2011
Published: November 23, 2011

can be performed in water at room temperature and without requiring any stringent condition.

It is known that larger NPs with diameter greater than 200 nm have short circulation time. In contrast, very small NPs (with diameter well below 10 nm) are removed rather quickly through renal clearance from the body systems. Therefore, a size between 10 to 200 nm should be optimal to achieve maximum stability as well as longer circulation time.[26] In fact it has been shown in the literature that a size range below 150 nm in diameter of NPs can be safely used for intravenous administration.[27]

We report here the coating of PEG of different molecular weights (1500, 4000, 10 000 and 20 000; represented as PEG1.5K, PEG4K, PEG10K and PEG20K, respectively, in the text) on Fe_3O_4 NPs of average size 8 ± 2 nm using sonication as the sole peptizing technique with high level of monodispersity keeping the hydrodynamic radii in the range of ∼70−140 nm in aqueous medium. We used sonication because this technique has been extensively used to generate novel materials, as a competitive alternative to other time-consuming preparation techniques.[28,29] In addition, we have also shown here that although the use of bare magnetic NPs can alter the redox state of cyt c, these PEG-coated NPs do not have any effect on the protein. We choose cyt c for the protein-NPs interaction study because it is an important heme containing metalloprotein and a key component of the electron transport chain inside mitochondria. Cyt c has been popularly used as a good model system to study protein-NP interaction[36,37] because of its small size, easy availability, and high stability in solution. Different aspects of cyt c biochemistry have been extensively studied using a variety of biophysical and spectroscopic methods.[38,39] The present experiments suggest that the interaction of bare Fe_3O_4 NPs with the oxidized state of the cyt c leads to the reduction of the heme group of the protein, whereas PEG-modified NPs do not show such behavior. Because any modification in the redox property of cyt c could potentially affect the energy production balance in the cell, this observation may have important implications on the use of magnetic NPs in the physiological systems.

2. EXPERIMENTAL SECTION

2.1. Materials. Ferric chloride hexahydrate ($FeCl_3·6H_2O$) and all the PEG polymers were obtained from Sigma-Aldrich, USA. Ferrous sulfate heptahydrate ($FeSO_4·7H_2O$) was purchased from MERCK, India. NaOH pellets were obtained from Sisco Research laboratory, India. Horse heart cyt c was purchased from Sigma, USA. Millipore water was used for the preparation of all the aqueous solutions.

2.2. Synthesis of the Bare and PEG-Coated Magnetic NPs. PEG-coated NPs were synthesized following a simple two-step coprecipitation approach. Initially, $FeSO_4·7H_2O$ and $FeCl_3·4H_2O$ were dissolved in water in 1:2 molar ratios under nitrogen protection. The resulting dark orange solution was stirred for 30 min at 60 °C. An aqueous NaOH solution (25%) was then added dropwise to the above hot solution with stirring over a period of 10 min. Instant color change from dark orange to black was found to occur with particle formation. Stirring was continued for further 30 min followed by cooling to room temperature. The solvent was removed by magnetic decantation. Washing of the particles was done several times with water to make the iron dispersion free of any residual salts, which was used during the coprecipitation. The final supernatant was decanted magnetically to obtain the as-prepared magnetite NPs. A 40 to 50% (w/v) aqueous solution of PEG of desired molecular weight (PEG1.5K, PEG4K, PEG10K, and PEG20K) was then added to the above as-prepared wet magnetic NPs and then sonicated for 1.5 min at room temperature with an ultrasonic probe (3 pulse of 30 s each, operated between 3−5 W). The supernatant was removed by centrifugation at 10 000 rpm and the solid product washed with water to remove unreacted PEG by magnetic separation. The final product was then dried at room temperature for several hours. The coated NPs will be represented as PEG1.5K-NPs, PEG4K-NPs, PEG10K-NPs, and PEG20K-NPs, respectively, in the text, for PEG1.5K, -4K, -10K, and -20K coating. Bare NPs without any PEG stabilization was prepared for comparison, following a similar procedure without the PEG addition step.

2.3. Preparation of Protein and NP Dispersions in Aqueous Buffer (pH 7.4). To disperse bare NPs, we adopted a literature method[40] with minor modification. To the freshly prepared solid NPs 200 μL of concentrated perchloric acid was added and then manually mixed for 10 min to obtain an acidic sol. This step was followed by peptization with water.[41] The water dispersion was then centrifuged at 10 000 rpm for 10 min to remove any insoluble particles. The final sample contained about 25 mg of Fe_3O_4 per ml as determined by ferrozine assay.[42] Briefly, 50 μL of the NP samples were diluted with distilled water to a final volume of 1 mL. NPs were then lysed by adding 0.5 mL of 1.2 mol HCl and 0.2 mL of 2 mol ascorbic acid. The reaction mixture was incubated for 2 h at 65−70 °C and then brought back to room temperature. Two-tenths of a millilter of a mixture of reagents (made with 6.5 mol of Ferrozine, 13.1 mmol of neocuproine, 2 mol of ascorbic acid, and 5 mol of ammonium acetate) was added to the above solution. After incubating for 30 min, the optical density of the sample was measured at 562 nm. Standard samples were prepared using ferrous ammonium sulfate (instead of NPs) of 0.0, 0.1, 0.2, 0.5, 1.0, 2.0, and 5.0 μg/mL to make the standard plot, from where the concentration of the NP sample was determined. A separate reaction mixture containing identical volume of water (without the NPs or the ferrous salt) was used as the blank.

As-prepared PEG-NPs were dispersed in buffer by vortexing thoroughly. In the case of PEG coated NPs the pH of the solution was maintained at 7.4 using sodium hydroxide to meet physiological limits. Five μmol cyt c solution was used for all the protein−NP interaction studies. The concentration of horse heart cyt c was determined using an extinction coefficient of 29 $mmol^{-1}$ cm^{-1} at 550 nm of the reduced protein. The protein was reduced using trace amount of sodium dithionite.

2.4. Characterizations. X-ray diffraction patterns of the solid powders were recorded with a Rigaku SmartLab X-ray diffractometer operating at 9 kW (200 mA x 45 kV) using Cu Kα (λ = 1.5406 Å) radiation. TG/DTA analyses of the solid samples were performed using a NETZSCH 409 C thermal analyzer. Samples were loaded in alumina crucible and measured at a rate of 5 °C min^{-1} between 40 to 600 °C. FTIR spectra of the solid samples were recorded by KBr pellet method using a Nicolet 380 FTIR spectrometer. Transmission electron microscopic (TEM) measurements were carried out using a Tecnai G^2 30ST (FEI) operating at 300 kV. Minimal amount of solid sample was dispersed in water−ethanol mixture (1:9 v/v) and small drops were placed on a carbon-coated copper grid. The grid was dried for 2−3 h in an air oven at 40 °C prior to the TEM studies. Magnetic measurements of the solid samples were performed using a Lakeshore-7407 vibrating sample magnetometer (VSM). UV−visible absorption spectroscopy measurements were performed in aqueous buffer using a Thermoscientific UV-10 spectrometer. Absorbance scans were taken from 200−800 nm using a quartz cuvette of 1 cm path length. Dynamic light scattering (DLS) measurements were performed with aqueous dispersions of PEG coated NPs using a Malvern Zetasizer Nano (model ZEN 3600). Far UV-CD spectra were recorded using a Jasco J715 spectropolarimeter (Japan Spectroscopic Ltd.). CD measurements were carried out with 5 μM protein using a 1 mm path length cuvette and a scan speed of 50 nm min^{-1}. Ten spectra were collected in continuous mode and averaged. A baseline correction with corresponding buffers was conducted for all the experiments.

3. RESULTS AND DISUSSIONS

3.1. General. PEG-coated Fe_3O_4 NPs samples are dark brown hygroscopic solids, and are readily dispersible in water to form stable and monodisperse solutions as confirmed by DLS

measurements. This result, at a first instance, gives an evidence of PEG coating, because bare Fe_3O_4 NPs are completely insoluble in water. The hydrodynamic diameters of the dispersed particles were found to be in the range between 70 and 140 nm. The size of the particles remained monodispersed (single DLS peak) up to 30 days (Figure 1), without any visible

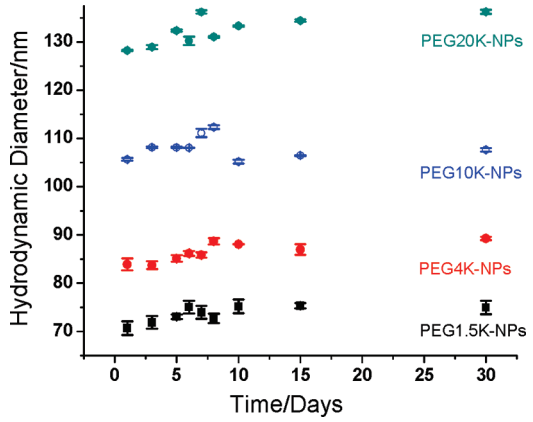

Figure 1. Change in hydrodynamic diameter for the PEG coated NPs in aqueous medium with respect to time (as measured by DLS). The molecular weights of PEGs are mentioned in the corresponding sample names. The error bars are calculated using three independent measurements. The particle sizes appeared to be almost unchanged up to 30 days in the dispersions.

precipitation. This reveals the highly stable nature of the PEG coated NPs in dispersions, which would be beneficial for biological studies where the NPs are needed to be stable in aqueous medium for longer time periods. NPs with PEG coatings of different molecular weights have shown magnetic property at room temperature. They are found to be readily attracted to a piece of magnet placed next to the powdered samples (Figure S1a, b in the Supporting Information). The aqueous solutions also show magnetic response at room temperature, the particles being attracted to the magnet from a homogeneous aqueous dispersion (Figure S1 c,d in the Supporting Information).

3.2. X-ray Diffraction Studies. The XRD measurements were performed with the dried powder samples of bare and PEG coated NPs to identify the crystal phases present in the samples. Figure 2 (panel A) shows the XRD pattern of a representative PEG coated Fe_3O_4 sample (PEG10K-NPs) (Figure 2A, curve a) along with bare (Figure 2A, curve b) Fe_3O_4 NPs and free PEG10K (Figure 2A, curve c). The pattern of the PEG10K-NPs (Figure 2A, curve a) showed all the major peaks corresponding to Fe_3O_4. The 2θ = 30.1, 35.5, 43.2, 57.2, 62.7, and 74.3 can be assigned to the (220), (311), (400), (511), (440), and (533) planes, respectively, of the Fe_3O_4 (JCPDS#19−0629), as also observed in case of bare NPs (Figure 2A, curve b). Additionally, one sharp peak around 2θ = 23° along with small peaks due to the PEG polymer are observed in the case of the PEG10K-NP (Figure 2A, curve a). This result confirmed the surface modification of the Fe_3O_4 NPs with PEG.

3.3. FTIR Measurements. To know about the modification of the NPs by the PEG molecules FTIR spectra were performed as solids dispersed in KBr matrix. The spectra of bare Fe_3O_4, free PEG20K and PEG20K-NPs are shown in Figure 2 (panel B). The bare Fe_3O_4 NPs showed characteristic

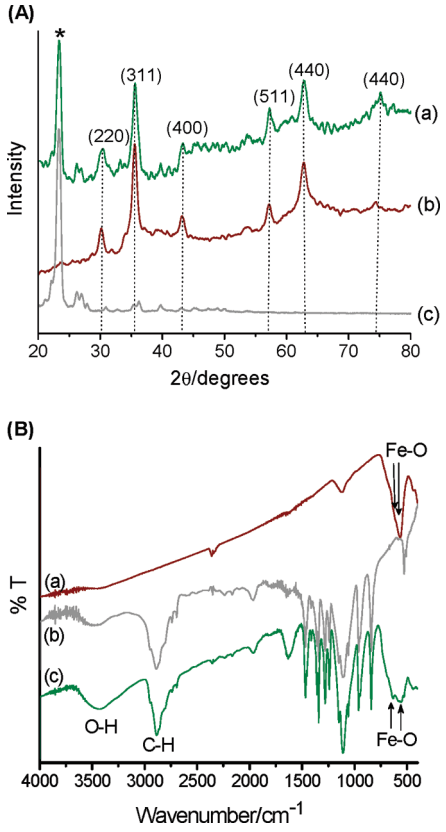

Figure 2. (A) XRD patterns of PEG10K-NPs (a), bare Fe_3O_4 NPs (b), and PEG10K (c). The symbol '★' represents the strongest PEG peak. (B) FT-IR spectra of the bare NPs (a), PEG20K (b), and PEG20K-NPs (c). The characteristic Fe−O stretching is shown by arrows. *Y* axes have been shifted for clarity.

bands related to the Fe−O vibrations near 618 (shoulder) and 569 cm^{-1} (Figure 2B, curve a).[26] Similar peaks have been observed in the spectra of the PEG20KNPs (at 633 and 569 cm^{-1}; Figure 2B, curve c), but not observed in that of solid PEG20K (Figure 2B, curve b).[30] Apart from that, a broad −O−H stretch around 3450 cm^{-1}, a sharp −C−H stretch around 2885 cm^{-1} and a sharp −C−O stretch around 1105 cm^{-1} are observed in both PEG and the PEG coated NPs (Figure 2B, curves b, c), revealing the presence of PEG residue in the final product. However these peaks are not observed in the spectrum of bare Fe_3O_4 NPs. These results clearly showed surface modification of Fe_3O_4 NPs with PEG.

3.4. TG/DTA Measurements. The presence of the PEG polymer in the final product has been further confirmed from the thermal analysis studies. The thermogravimetry (TG) curves of two PEG coated samples PEG20K-NPs and PEG4K-NPs and one differential thermal analysis (DTA) curve of PEG4K-NPs are shown in Figure 3 as representatives. The TG curves of PEG4K-NPs and PEG20K-NPs (Figure 3a,b) showed a small endothermic weight loss of about 1% within the first 125 °C. This can be correlated to the loss of the water molecules. The next small weight gain (∼1%) in the temperature range of 125−155 °C (this portion of TG curves are shown in the inset with magnified scale) could be attributed to the thermal conversion of Fe_3O_4 to γ-Fe_2O_3.[43] This small weight gain is due to the increase in oxygen content during the thermal conversion of Fe_3O_4 to Fe_2O_3 (2 Fe_3O_4 → 3 γ-Fe_2O_3). For this conversion the DTA of PEG4K-NPs shows an

dx.doi.org/10.1021/am201166m | ACS Appl. Mater. Interfaces 2012, 4, 142−149

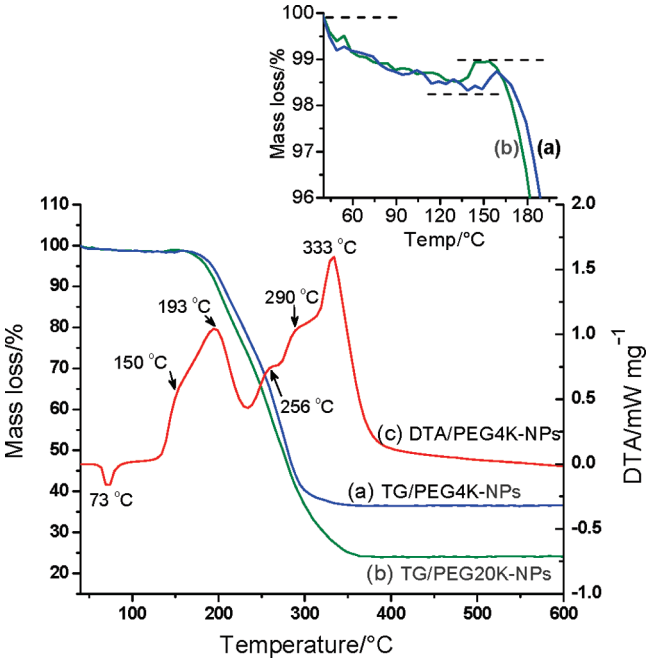

Figure 3. Thermal studies showing the TG curves for PEG4K-NPs (a), PEG20K-NPs (b); and DTA curve of PEG4K-NPs (c). Inset shows the mass loss of a and b in expanded scale in the temperature range 40−200 °C. The % mass losses are consistent with the molecular weight of the PEG molecule.

exothermic peak at ∼150 °C (Figure 3c). In addition, a multistep exothermic weight loss has been observed (between 175 and 350 °C) because of the decomposition of PEG fractions. This large weight loss step accounts for ∼60 and 80% mass loss for the PEG4K-NPs and PEG20K-NPs, respectively. Relatively large weight loss in the latter case is due to the high molecular weight of the PEG20K. After 350 °C, there was practically no change in weight throughout the temperature range up to 600 °C (Figure 3a,b).

3.5. TEM Study. Transmission electron microscopy (TEM) was performed for both bare and PEG-coated NPs to learn the details of the structure. TEM images of the bare Fe_3O_4 NPs are shown in Figure S2 in the Supporting Information. The low-resolution image (see Figure S2a in the Supporting Information) shows existence of spherical NPs of about 8−10 nm in size. The corresponding high-resolution image (see Figure S2b in the Supporting Information) shows clear lattice fringes corresponding to magnetite (Fe_3O_4). The EDX and SAED patterns (see Figure S2c,d in the Supporting Information) are also in consistent with the presence of (Fe_3O_4). TEM images of one representative PEG coated sample (PEG4K-NPs) are shown in Figure 4a−d. It was observed from the low-resolution bright field image (Figure 4a) that the PEG-encapsulated NPs are mostly spherical with an average size around 8 nm, similar to bare NPs. However, there are multiple numbers of NPs present as the core inside large PEG encapsulations. It seems that several NPs remain attached together as aggregates by mutual magnetic attractions to form the cores. It is difficult to achieve the high-resolution image of the individual NPs through the thick PEG encapsulation and also the lattice fringes on the particles and the surroundings. However, one major crystal plane for both magnetite (220) and PEG could be identified from the high resolution TEM, and are marked in the Figure 4b. The EDX (Figure 4c) has shown the

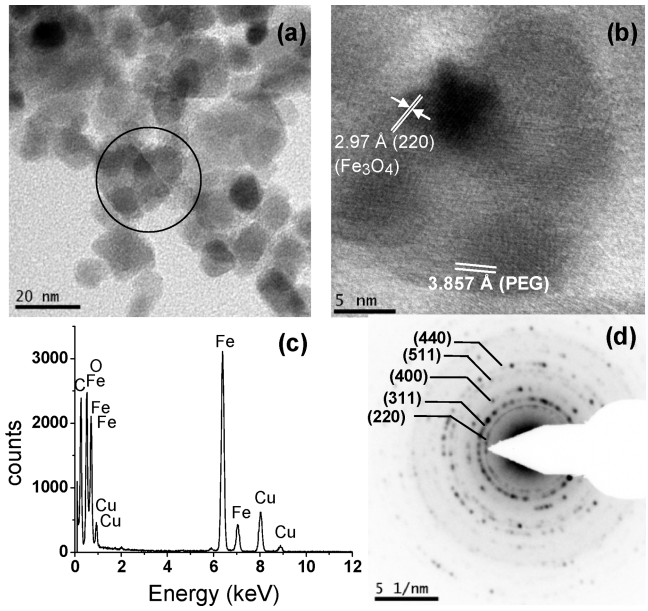

Figure 4. TEM of PEG4K-NPs showing (a) bright-field image, (b) HRTEM of the circled part of a, (c) EDX, and (d) SAED pattern.

presence of Fe, O, C and Cu. The Cu peaks are from the copper grid used for TEM studies. O and a part of C are from the PEG of the sample. The SAED pattern (Figure 4d) is complicated with large number of spots indicating aggregations in various places. Although most of the rings/spots from Fe_3O_4 could be identified, identifications of PEG could not be achieved from the SAED because the strongest PEG line appears closer to the central bright zone of SAED (Figure 4d).

3.6. Magnetic Property Measurements. PEG-coated NPs have exhibited good magnetic response and are easily attracted to a magnet placed beside as shown in Figure S1 in the Supporting Information. The magnetization curves for two representatives PEG coated NPs are shown in Figure 5.

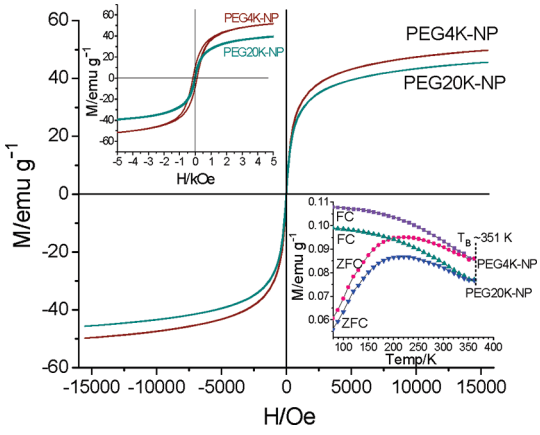

Figure 5. Magnetization response with increasing and decreasing applied magnetic field for PEG-coated NPs at 300 K. Top and bottom insets show the hysteresis loops at 80 K and the FC/ZFC curves with increasing temperature, respectively.

Corresponding magnetization curves measured in similar experimental conditions for the bare NPs are provided in the Supporting Information for comparison (Figure S3). The magnetic field vs moment ($M-H$) measurements of the solid samples are performed at both 300 K (room temperature) and

dx.doi.org/10.1021/am201166m | ACS Appl. Mater. Interfaces 2012, 4, 142−149

80 K with the magnetic field swept back and forth between +20 and −20 kOe. The saturation magnetic moments obtained are 50 and 43 emu g^{-1} at 300 K, and 60 and 46 emu g^{-1} at 80 K, for PEG4K-NPs and PEG20K-NPs respectively, as shown in the Figure 5. However, the saturation magnetic moment values for the bare NPs are found to be 140 and 160 emu g^{-1} at 300 and 80 K, respectively. The hysteresis loops of the samples are shown in the top insets of Figure 5 and Figure S3 in the Supporting Information). Although the coercivity value obtained for bare Fe_3O_4 at 300 K is ~330 Oe, no hysteresis loop is observed in either of the coated NPs (Figure 5). However, at 80 K, the PEG4K-NPs show a value of ~260 Oe, whereas PEG20K-NPs show a very low coercivity (~42 Oe) (Figure 5; top inset). In contrast, bare NPs have shown a high coercive field of ~650 Oe at 80 K (Figure S3, top inset, in the Supporting Information). Therefore, a significant softening of magnetic property has occurred because of the PEG-coating onto the Fe_3O_4 NPs. It is known that any change in the magnetic properties of NPs primarily depends on two major factors: (i) change in size and (ii) change in the surface state.[44] Since no significant size change has occurred due to PEG coating (as observed from both TEM and XRD results, discussed in the previous sections), the changes in the magnetic properties can be attributed to the surface modifications by large PEG polymer molecules. The bottom inset of Figure 5 has shown the temperature dependence of the magnetization for the field-cooled (FC) and zero-field-cooled (ZFC) curves for the PEG4K-NPs and PEG20K-NPs. It is observed from the figure that FC and ZFC magnetization curves are split below the block temperature (T_B, the transformation temperature from ferromagnetism to superparamagnetisam), and they merge each other above T_B.[45] In all our samples, the T_B lies above the room temperature (~351 K for PEG4K-NPs and PEG20K-NPs and 362 K for bare Fe_3O_4 NPs; see bottom insets of Figure 5 and Figure S3 in the Supporting Information), which further explains the room temperature ferromagnetism of these NPs. It can be also said from the T_B point of view that softening of magnetic property has occurred from bare to coated NPs.

A notable feature in case of PEG4K- and PEG20K coated NPs is that along with the decrease of magnetization with temperature in the FC curve, the corresponding ZFC curve displays a maximum around 225 K (Figure 5; bottom inset). This effect was not observed in case of bare Fe_3O_4. Probably due to the absence of the surface polymers the moment value of bare NPs increases uniformly until it reached T_B (see Figure S3, bottom inset, in the Supporting Information). In the light of the above discussion the PEG coated NPs can be considered as moderately soft magnetic materials compared to the bare Fe_3O_4 NPs. As soft magnetic materials are especially important in the biomedical fields,[46] these PEG-coated soft magnetic NPs may find good applications in the biological studies. In the later section we shall discuss the interactions of these coated NPs with an electron transport protein cyt c.

3.7. Interaction of Bare and PEG-Coated Fe_3O_4 NPs with Cytochrome C. UV−visible absorption spectroscopy has been used to study the effect of bare and PEG-coated Fe_3O_4 NPs on cyt c. Figure 6 shows the UV−visible absorption spectra of cyt c in the absence and presence of both bare and PEG10K-NPs. The native state of cyt c (in sodium phosphate buffer at pH 7.4 in the absence of NPs) is characterized by the Soret peak at 409 nm and a small peak at 528 nm as shown in Figure 6 (gray curve). These absorption peaks originates due to

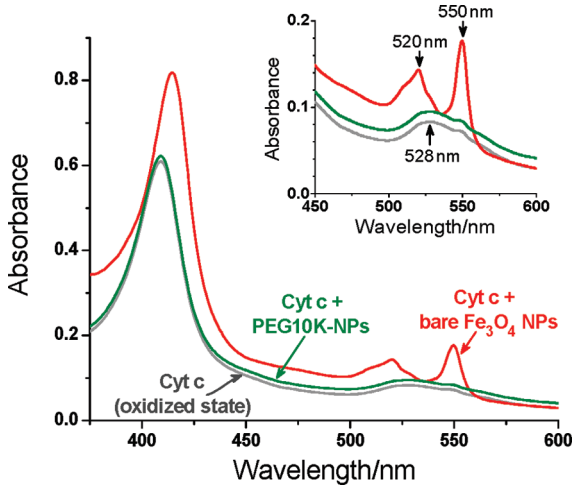

Figure 6. UV−visible spectra showing the reduction of cyt c in the presence of bare Fe_3O_4 NPs (red curve). The native oxidized state of cyt c (gray curve) remains unaffected in the presence of PEG10K-NPs (olive green curve). The inset shows expanded scale of the region 450−600 nm.

the presence of porphyrin chromophore in the protein and represent the oxidized state of the protein. Immediately after the addition of bare NPs, the Soret band shifts to 414 nm (Figure 6; red curve) and the broad peak at 528 nm disappears with the evolution of two well-defined absorption peaks at 520 and 550 nm (Figure 6; red curve; also shown in a magnified scale as inset). The appearance of Soret peak at 414 nm and the double peaks at 520 and 550 nm in the visible region are the typical characteristics of the reduced state of cyt c and this spectral feature match very well with the absorption spectrum of cyt c reduced using trace amount of sodium dithionite (see Figure S4 in the Supporting Information). This data suggests that the interaction of bare NPs with cyt c leads to the reduction of the protein. Similar experiments (performed in identical experimental conditions) with PEG10K coated Fe_3O_4 NPs (PEG10K-NPs) do not show any change in the spectra of the oxidized state of the protein (like in Figure 6; olive green curve). To understand if the molecular weight of PEG has any observable effect, the experiments have been carried out with Fe_3O_4 NPs coated with different molecular weights (1.5K, 4K, 10K, and 20K). No reduction has been observed in any of these cases. Rather, PEGs of different molecular weights have been found very similar in their behavior toward the prevention of cyt c reduction at least in the time frame of our study (about 30 min for these measurements, Figure S5a in the Supporting Information). A time-dependent study has also been performed to determine if the presence of PEG10K coating with the Fe_3O_4 NPs actually prevents the reduction of cyt c, or it merely slows down the reduction kinetically. The data shown in Figure S5b (see the Supporting Infomration) confirm the absence of any significant reduction of cyt c even after incubating the protein for 2 h in the presence of PEG10K-NPs. As a matter of fact, no reduction has been observed when the samples have been incubated for 24 h at room temperature although the presence of background scattering is observed presumably because of the aggregation of cyt c.

It can be noted here that in the presence of bare NPs, the reduction phenomenon of cyt c occurs without any change in the secondary structure of the protein. There are several precautionary measures, which have been taken to make sure

dx.doi.org/10.1021/am201166m | ACS Appl. Mater. Interfaces 2012, 4, 142−149

that the reduction of the protein observed by the addition of Fe_3O_4 NPs is real, and not an artifact arising from other factors including solution and buffer conditions. This is particularly important because perchloric acid has been used for peptization whose presence at low concentration may result in the decrease in pH. This decrease in pH may in turn affect the conformational integrity of the protein and thus leading to its reduction. In essence, it is important to find out whether the observed reduction is a true effect of the Fe_3O_4 NPs or is it just a manifestation of low pH induced conformational change of the protein. To further address this concern experimentally, we have carried out far UV circular dichroism measurements (far UV CD) with cyt c at different pH values between 7.4 and 4.5 by adding perchloric acid and the data are shown in Figure 7.

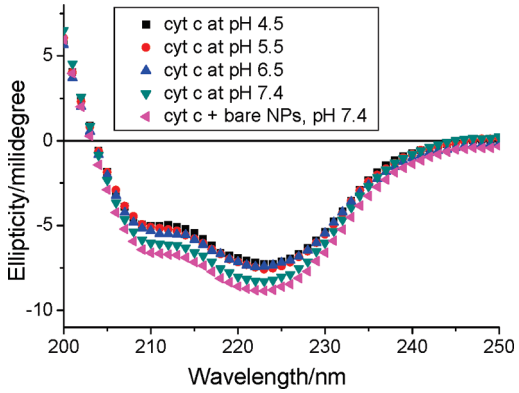

Figure 7. Far UV CD spectra of cyt c at different pH solutions (pH values are mentioned in the Figure), along with the spectrum of the native protein in the presence of bare Fe_3O_4 NPs at pH 7.4, measured in identical solution condition. Absence of any significant difference in all the above CD spectra indicate that there is no appreciable change in the secondary structure of the protein either in the presence of bare NPs, or by lowering the pH of the medium. However, the reduction of heme group takes place in the presence of bare NPs at pH 7.4 (as shown in Figure 6).

Circular dichroism is chosen for these experiments since it is an efficient and widely accepted technique for monitoring the conformation of proteins. Two negative peaks at 222 nm and at 209 nm are observed, which is characteristic of the alpha helical nature of cyt c. The far UV CD spectra of the protein remain essentially identical in the pH range studied (between 7.4 and 4.5) (Figure 7) indicating no significant change in the secondary structure of the protein. The data indicates that the presence of trace amount of perchloric acid (if any) should not lead to any major structural or conformational disorientation of cyt c. Also reported in the same figure (Figure 7), is the far UV CD of cyt c in the presence of Fe_3O_4 NPs at identical solution condition where reduction is observed (as shown in Figure 6, red curve). No change in the secondary structure has been observed in the presence of Fe_3O_4 NPs, though the reduction of the protein has taken place immediately after the addition. These data prove beyond doubt that the observed reduction is an effect associated with the presence of NPs without affecting the native conformation of the protein. It is nevertheless important to point out that all our experiments have been carried out using buffer solutions maintained strictly at pH 7.4.

The interaction of cyt c with bare and PEG-coated Fe_3O_4 NPs is shown schematically in Figure 8. A bioinformatics

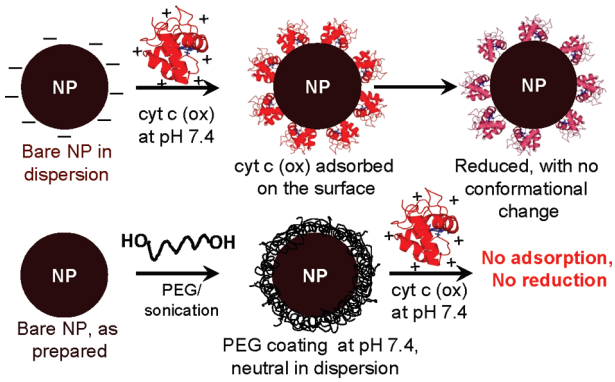

Figure 8. Schematic representation of the interaction of cyt c with the bare and PEG coated Fe_3O_4 NPs. In the case of bare NPs, the protein is adsorbed onto the surface of NPs by electrostatic interactions, followed by immediate reduction of the heme group. The presence of PEG coating resists cyt c adsorption on the surface and hence the reduction is not observed. Wine red and pink colors of the native oxidized and reduced cyt c, respectively, were chosen as per the colors of the actual aqueous solutions of the two forms of the protein.

analysis of the sequence of cyt c using ProtParam,[47] suggests that the protein is positive (total charge of +8), while the surface of the Fe_3O_4 NPs is highly negative (the zeta potential is measured as −30 mV) at pH 7.4. Therefore, the interaction of cyt c with the surface of the Fe_3O_4 NPs at pH 7.4 is electrostatically favored. However, it is observed that at pH 4.5 cyt c and bare Fe_3O_4 NPs are both positively charged (measured zeta potentials for cyt c and the bare NPs are +8 and +36 mV, respectively) and hence any interaction between them, if guided by electrostatics, would be disfavored. To strengthen our observation, we have designed a control experiment where the bare Fe_3O_4 NPs are added to a solution of cyt c at pH 4.5, the result of which is shown in Figure S6 in the Supporting Information. The UV−visible absorption shows absolutely no reduction of cyt c at pH 4.5. Hence it can be assumed that the reduction of cyt c by bare NPs is electrostatically dependent on the pH of the medium. While an extensive investigation on the interaction between the protein and Fe_3O_4 NPs is being worked out in our laboratory using several biophysical and spectroscopic techniques, the above experimental observations show that the electrostatics can play very important roles in the initial adsorption of the protein on the bare NP surface. As PEG is known to resist protein adsorption,[48] no interaction of cyt c with the Fe_3O_4 core is possible in case of PEG-coated NPs. This effect of PEG should be responsible for the lack of interaction (or adsorption) of cyt c with the PEG-coated Fe_3O_4 NPs at pH 7.4.

Although the mechanism of cyt c reduction is not yet identified, two possibilities could be considered. First, the reduction of the protein may have originated from the oxidation affinity of the bare NPs from magnetite (mixture of Fe^{2+} and Fe^{3+}) to maghemite (all Fe^{3+}) giving away one electron to the protein that is adsorbed on the surface,[49] leading to its reduction. The second possibility originates from the numerous reports of magnetic NPs induced generation of reactive oxygen species including superoxide radicals.[50]

The first mechanism is expected to be relatively noninvasive toward the conformation and stability of the protein. This is because the reduced protein has been shown to have higher conformational stability compared to its oxidized state.[51] However, there is always a possibility of unfolding as a result

dx.doi.org/10.1021/am201166m | ACS Appl. Mater. Interfaces 2012, 4, 142−149

of protein adsorption on NPs surface. The second mechanism, on the other hand, may generate conformationally unstable protein. This is because the generated reactive oxygen species, besides reducing cyt c, may attack the protein nonspecifically leading to structural and conformational degeneration. Experiments are underway in our laboratory using a number of biophysical and spectroscopic methods to study different aspects of conformation and stability of cyt c in the presence of Fe_3O_4 NPs to identify the relevant mechanism.

With the advancement of nanoparticle -induced drug delivery methods and nanomedicines, protein−NP interaction has recently attracted significant attention. A potential therapeutic application of bare Fe_3O_4 NPs has been reported that shows its effects to inhibit lysozyme aggregation.[40] Also the use of bare and coated Fe_3O_4 NPs as potential models of peroxidases has been shown.[52] While the biological applications of magnetic NPs are increasing at a rapid pace, the present study emphasizes on the potential toxicity of these particles and the importance of using efficient surface modification systems to minimize their toxic effects. Moreover, the softer magnetic nature of the PEG coated particles, compared to the bare Fe_3O_4 NPs, makes them especially useful for biological studies, where a stronger magnetic property may be harmful for the system. Therefore, the present study strongly suggests that the surface modification of bare Fe_3O_4 by PEG molecules not only reduces the possibility of oxidation but also softens the strong magnetic nature of the NPs significantly.

4. CONCLUSION

We report here a fast and easy green synthetic route for the preparation of Fe_3O_4 NPs coated with PEG molecules of different molecular weight. The highly water dispersible coated NPs of suitable hydrodynamic radii are stable in aqueous medium and possess a moderately soft magnetic nature at room temperature, which could be an essential feature to use these as biomedically important magnetic materials. Although the interaction of bare NPs with horse heart cyt c leads to reduction of the protein, PEG-coated magnetite NPs do not show this behavior. This could very well be a protective measure to be taken while working with magnetic NPs in biological systems, where the protection of biomolecules will be necessary from the toxicity generated by the magnetic NPs. Such a specific protective effect of PEG coatings on magnetite NPs, toward the redox property of any metalloprotein, has been experimentally shown for the first time.

■ ASSOCIATED CONTENT

Ⓢ Supporting Information

Room-temperature magnetic response of PEG10K-NPs (solid and water dispersed) (Figure S1), TEM images of the bare magnetite NPs (Figure S2), magnetic measurements of bare magnetite NPs (Figure S3), UV−visible studies of native oxidized and dithionite reduced state of cyt c (Figure S4), UV−visible absorbance spectra of the native oxidized cyt c in the presence of different PEG-coated NPs up to 30 min incubation (Figure S5a) and the time-study up to 120 min in presence of PEG10K-NPs at pH 7.4 (Figure S5b), and UV−visible absorbance scan of cyt c in the presence of bare Fe_3O_4 NPs at pH 4.5 (Figure S6). This material is available free of charge via the Internet at http://pubs.acs.org.

■ AUTHOR INFORMATION

Corresponding Author

*Tel: +91 33 24733469/96, ext. 3403. Fax: 91-33-24730957. E-mail: gde@cgcri.res.in.

Author Contributions

‖These authors have contributed equally to this research.

■ ACKNOWLEDGMENTS

Financial support from the Department of Science and Technology (DST), Government of India, under National Nano Misson programme (Grant SR/S5/NM-17/2006) is thankfully acknowledged. K.C. acknowledges financial support from the EMPOWER project grant (#OLP004) provided by CSIR. A.M. and N.J. thank CSIR for awarding a Research Associateship and Project Assistantship, respectively.

■ REFERENCES

(1) Qiao, R.; Yang, C.; Gao, M. *J. Mater. Chem.* **2009**, *19*, 6274−6293.
(2) Lee, H.; Lee, E.; Kim, D. K..; Jang, N. K.; Jeong, Y. Y.; Jon, S. *J. Am. Chem. Soc.* **2006**, *128*, 7383−7389.
(3) Babic, M.; Horák, D.; Trchová, M.; Jendelová, P.; Glogarová, K.; Lesný, P.; Herynek, V.; Hájek, M.; Syková, E. *Bioconjugate Chem.* **2008**, *19*, 740−750.
(4) Druet, E.; Mahieu, P.; Foidart, J. M.; Druet, P. *J. Immunol. Methods* **1982**, *48*, 149−157.
(5) Gupta, A. K.; Gupta, M. *Biomaterials* **2005**, *26*, 3995−4021.
(6) Fortin, J.; Wilhelm, C.; Servais, J.; Ménager, C.; Bacri, J.; Gazeau, F. *J. Am. Chem. Soc.* **2007**, *129*, 2628−2635.
(7) Torchilin, V. P. *Eur. J. Pharm. Sci.* **2000**, *11*, S81.
(8) Xuan, S.; Wang, F.; Lai, J. M. Y.; Sham, K. W. Y.; Wang, Y-X. J.; Lee, S.-F.; Yu, J. C.; Cheng, C. H. K.; Leung, K. C-F. *ACS Appl. Mater. Interface* **2011**, *3*, 237−244.
(9) Vonk, G. P.; Schram, J. L. *J. Immunol. Methods* **1991**, *137*, 133−139.
(10) Nam, J. M.; Thaxton, C. S.; Mirkin, C. A. *Science* **2003**, *301*, 1884−1886.
(11) Bhirde, A.; Xie, J.; Swierczewska, M.; Chen, X. *Nanoscale* **2011**, *3*, 142−153.
(12) Maynard, A. D.; Aitken, R. J.; Butz, T.; Colvin, V.; Donaldson, K.; Oberdorster, G. *Nature* **2006**, *444*, 267−269.
(13) Mahmoudi, M.; Simchi, A.; Imani, M.; Milani, A. S.; Stroeve, P. *Nanotechnology* **2009**, *20*, 225104.
(14) Karlsson, H. L.; Gustafsson, J.; Cronholm, P.; Moller, L. *Toxicol. Lett.* **2009**, *188*, 112−118.
(15) Stevens, R. G.; Jones, D. Y.; Micozzi, M. S.; Taylor, P. R. *N. Engl. J. Med.* **1988**, *319*, 1047−1052.
(16) Toyokuni, S. *Free Radical Biol. Med.* **1996**, *20*, 553−566.
(17) Toyokuni, S. *Redox Rep.* **2002**, *7*, 189−197.
(18) Valko, M.; Leibfritz, D.; Moncol, J.; Cronin, M. T.; Mazur, M.; Telser, J. *Int. J. Biochem. Cell Biol.* **2007**, *39*, 44−84.
(19) Dave, S. R.; Gao, X. *Nanomed. Nanobiotechnol.* **2009**, 1583−1609.
(20) Lutz, J. F.; Stoller, S.; Hoth, A.; Kaufner, L.; U. Pison, U.; Cartier, R. *Biomacromolecules* **2006**, *7*, 3132−3138.
(21) López-Cruz, A.; Barrera, C.; Calero-Ddelc, V. L.; Rinaldi, C. *J. Mater. Chem.* **2009**, *19*, 6870−6876.
(22) Il Park, Y.; Piao, Y.; Lee, N.; Yoo, B.; Kim, B. H.; Choi, S. H.; Hyeon, T. *J. Mater. Chem.* **2011**, *21*, 11472−11477.
(23) Mao, S.; Neu, M.; Germershaus, O.; Merkel, O.; Sitterberg, J.; Bakowsky, U.; Kissel, T. *Bioconjugate Chem.* **2006**, *17*, 1209−1218.
(24) Conover, C. D.; Greenwald, R. B.; Pendri, A.; Gilbert, C. W.; Shum, K. L. *Cancer Chemother. Pharmacol.* **1998**, *42*, 407−414.
(25) Zhou, L.; Yuan, J.; Wei, Y. *J. Mater. Chem.* **2011**, *21*, 2823−2840.
(26) Gupta, A. K.; Wells, S. *IEEE Trans. Nanosci.* **2004**, *3*, 66−73.

(27) Bautista, M. C.; Bomati-Miguel, O.; Del Puerto Morales, M. *J Magn. Magn. Mater.* **2005**, *293*, 20−27.
(28) Cohen, H.; Gedanken, A.; Zhong, Z. *J. Phys. Chem. C* **2008**, *112*, 15429.
(29) Theerdhala, S.; Bahadur, D.; Vitta, S.; Perkas, Z.; Zhong, Z.; Gedanken, A. *Ultrason. Sonochem.* **2010**, *17*, 730.
(30) Park, J. Y.; Patel, D.; Lee, G. H.; Woo, S.; Chang, Y. *Nanotechnology* **2008**, *19*, 365603.
(31) Zhang, J.; Rana, S.; Srivastava, R. S.; Misra, R. D. K. *Acta Biomater.* **2008**, *4*, 40−48.
(32) Hu, F.; MacRenaris, K. W.; Waters, E. A.; Liang, T.; Schultz-Sikma, E. A.; Eckermann, A. L.; Meade, T. J. *J. Phys. Chem. C* **2009**, *113*, 20855−20860.
(33) Lee, H.; Lee, E.; Kim, D. K.; Jang, N. K.; Jeong, Y. Y.; Jon, S. *J. Am. Chem. Soc.* **2006**, *128*, 7383−7389.
(34) Amici, J.; Allia, A.; Tiberto, P.; Sangermano, M. *Macromol. Chem. Phys.* **2011**, *212*, 1629−1635.
(35) Hu, F. Q.; Wei, L.; Zhou, Z.; Ran, Y. L.; Li, Z.; Gao, M. Y. *Adv. Mater.* **2006**, *18*, 2553−2556.
(36) Jensen, P. S.; Chi, Q.; Grumsen, F. B.; Abad, J. M.; Horsewell, A.; D. J. Schiffrin, D. J.; Ulstrup, J. *J. Phys. Chem. C* **2007**, *111*, 6124−6132.
(37) Bayraktar, H.; You, C. C.; Rotello, V. M.; Knapp, M. J. *J. Am. Chem. Soc.* **2007**, *129*, 2732−2733.
(38) Gray, H. B.; Winkler, J. R. *Annu. Rev. Biochem.* **1996**, *65*, 537−561.
(39) Halder, S.; Mitra, S.; Chattopadhyay, K. *J. Biol. Chem.* **2010**, *285*, 25314−25323.
(40) Bellova, A.; Bysstrenova, E.; Koneracka, M.; Kopcansky, P.; Valle, F.; Tomasovicova, N.; Timko, M.; Bagelova, J.; Biscarim, F.; Gazova, Z. *Nanotechnology* **2010**, *21*, 065103.
(41) Because perchloric acid is corrosive and its presence in trace amount in solution could affect biomolecules including proteins, several control experiments were carried out to confirm the structural integrity of the studied protein, which are all discussed in section 3.7.
(42) Balivada, S.; Rachakatla, R. S.; Wang, H.; Samarakoon, T. N.; Dani, R. K.; Pyle, M.; Kroh, F. O.; Walker, B.; Leaym, X.; Koper, O. B.; Tamura, M.; Chikan, V.; Bossmann, S. H.; Troyer, D. L. *BMC Cancer* **2010**, *10*, 119−127.
(43) Lepp, H. *Am. Mineral.* **1957**, *42*, 679−681.
(44) Tan, Y.; Zhuang, Z.; Peng, Q.; Li, Y. *Chem. Mater.* **2008**, *20*, 5029−5034.
(45) Chatterjee, J.; Haik, Y.; Chen, C. J. *J. Magn. Magn. Mater* **2003**, *257*, 113−118.
(46) Wang, Z.; Zhu, H.; Wang, X.; Yang, F.; Yang, X. *Nanotechnology* **2009**, *20*, 465606.
(47) Gasteiger, E.; Hoogland, C.; Gattiker, A.; Duvaud, S.; Wilkins, M. R.; Appel, R. D.; Bairoch, A. Waker, J. M., Eds. *The Proteomix Protocols Handbook*; Humana Press: New York, 2005; pp 571−607.
(48) Verma, A.; Stellacci, F. *Small* **2010**, *6*, 12−21.
(49) Laurent, S.; Forge, D.; Port, M.; Roch, A.; Robic, C.; Vander Elst, L. *Chem. Rev.* **2008**, *108*, 2064−2011.
(50) Dikalov, S.; Griendling, K. K.; Harrison, D. G. *Hypertension* **2007**, *49*, 717−727.
(51) Latypov, R. F.; Maki, K.; Cheng, H.; Luck, S. D.; Roder, H. *J. Mol. Biol.* **2008**, *383*, 437−453.
(52) Gao, L.; Zhuang, J.; Nie, L.; Zhang, J.; Zhang, Y.; Gu, N. *Nature Nanotechnol.* **2007**, *2*, 77−583.